© 2006, Proceedings of the First International Conference on the
Application of Physical Modelling to Port and Coastal Protection. ISBN xxx-xxxx-xx-x

WAVE FORCES AND MOMENTS ON HEAVILY OVERTOPPED VERTICAL CURRENT DEFLECTION DIKE

STEVEN A. HUGHES [1], HARLEY S. WINER [2] & EDWARD R. BLODGETT [3]

[1] *Senior Research Engineer, Coastal and Hydraulics Laboratory, U.S. Army Corps of Engineers 3909 Halls Ferry Road, Vicksburg, MS 39180, USA. Steven.A.Hughes@erdc.usace.army.mil*

[2] *Chief, Coastal Engineering Section, New Orleans District, U.S. Army Corps of Engineers, 7400 Leake Avenue, New Orleans ,LA 70118, USA. Harley.S.Winer@mvn02.usace.army.mil*

[3] *Hydraulic Engineer, Coastal Engineering Section, New Orleans District, U.S. Army Corps of Engineers, 7400 Leake Avenue, New Orleans, LA 70118, USA. Edward.R.Blodgett@mvn02.usace.army.mil*

Abstract

Irregular wave forces on a heavily overtopped thinned-wall vertical current deflection dike were measured during a series of laboratory experiments. The purpose of the experiments was to obtain site-specific engineering values for use in design of a dike located at the mouth of the Mississippi River and to develop generic design guidance for heavily overtopped vertical walls. Predictive equations for the root-mean-squared shoreward-directed peak total force and associated moment arm were developed in terms of the incident wave momentum flux and relative wall height.

1. Introduction and Background

The focus of this study was a vertical, thin-wall dike located at the mouth of the Southwest Pass channel of the Mississippi River in Louisiana, USA. The dike extends perpendicular from the west river jetty approximately 245 m (800 ft) into the river as shown on Figure 1, and its function is to divert river flow toward the main navigation channel to help prevent channel shoaling. Water depths along the dike range up to 6.4 m (21 ft). The most recent wooden dike structure suffered extensive wave damage annually, and it is to be replaced with a new steel vertical wall having a top elevation either near or below Gulf mean lower low water (mllw) level. Thus, during storms the wall will be heavily overtopped, with the upper portion of storm waves passing over the wall. River currents in the upper few meters of the water column will not be diverted by the dike, but instead will continue to flow seaward over the wall and act as an opposing current on the incoming wave crests. The objectives of this study were (1) to determine specific force and moment loading on the wall for design of this specific structure, and (2) to develop generic design guidance applicable for similar situations.

Placing the top of the dike at an elevation comparable to the incoming wave trough introduces several hydrodynamic complexities. The dike will be heavily overtopped during storm conditions, and the overflowing water will cause a region of flow separation and lower pressure on the leeside of the wall (Knott and Mackley 1980). This low pressure will increase the shoreward-directed wave force at the top of the wall. Incoming waveform characteristics

Report Documentation Page

Form Approved
OMB No. 0704-0188

1. REPORT DATE	2. REPORT TYPE	3. DATES COVERED
2006		**00-00-2006 to 00-00-2006**

4. TITLE AND SUBTITLE	5a. CONTRACT NUMBER
Wave Forces and Moments on Heavily Overtopped Vertical Current Deflection Dike	5b. GRANT NUMBER
	5c. PROGRAM ELEMENT NUMBER
6. AUTHOR(S)	5d. PROJECT NUMBER
	5e. TASK NUMBER
	5f. WORK UNIT NUMBER
7. PERFORMING ORGANIZATION NAME(S) AND ADDRESS(ES) **U.S. Army Corps of Engineers,Coastal and Hydraulics Laboratory,3909 Halls Ferry Road,Vicksburg,MS,39180-6199**	8. PERFORMING ORGANIZATION REPORT NUMBER
9. SPONSORING/MONITORING AGENCY NAME(S) AND ADDRESS(ES)	10. SPONSOR/MONITOR'S ACRONYM(S)
	11. SPONSOR/MONITOR'S REPORT NUMBER(S)

12. DISTRIBUTION/AVAILABILITY STATEMENT
Approved for public release; distribution unlimited

13. SUPPLEMENTARY NOTES
Proceedings of the First International Conference on the Application of Physical Modelling to Port and Coastal Protection, 8-10 May 2006, Porto, Portugal

14. ABSTRACT
Irregular wave forces on a heavily overtopped thinned-wall vertical current deflection dike were measured during a series of laboratory experiments. The purpose of the experiments was to obtain site-specific engineering values for use in design of a dike located at the mouth of the Mississippi River and to develop generic design guidance for heavily overtopped vertical walls. Predictive equations for the root-mean-squared shoreward-directed peak total force and associated moment arm were developed in terms of the incident wave momentum flux and relative wall height.

15. SUBJECT TERMS

16. SECURITY CLASSIFICATION OF:			17. LIMITATION OF ABSTRACT	18. NUMBER OF PAGES	19a. NAME OF RESPONSIBLE PERSON
a. REPORT	b. ABSTRACT	c. THIS PAGE			
unclassified	**unclassified**	**unclassified**	**Same as Report (SAR)**	**10**	

will be altered by both the partial wave reflection at the wall, and by the out-flowing river current that will steepen the incident wave crests to some degree.

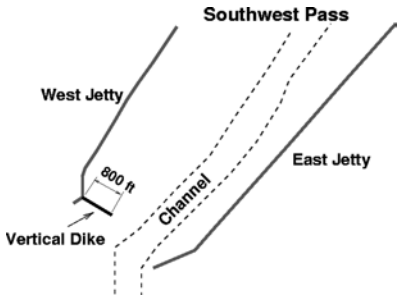

Figure 1. Current deflection dike location at the mouth of the Mississippi River

2. Experiments, Measurements, and Analyses

2.1 Experiment Parameters. Experiments were conducted in a large basin at a geometrically undistorted length scale of 1:50 with hydrodynamics and measured forces scaled according to Froude similarity. This length scale was chosen to best suit an existing experimental setup in the tidal inlet simulation facility at the Coastal and Hydraulics Laboratory in Vicksburg, Mississippi, USA. The vertical dike was situated in the basin similar to shown in Figure 1. However, in the model the east jetty did not extend as far seaward as in the prototype.

The key parameters for the experiments (in prototype-scale units) are as follows. Water elevation was held constant at +0.55 m mllw and the seafloor elevation at the wall was –6.7 m mllw giving a total water depth of 7.25 m for all experiments. Offshore depth at the plunger-type wavemaker was 15.8 m. Four wall heights were tested having top elevations of -1.83 m, -0.91 m, +0 m, and +0.91 m mllw. Top wall elevations relative to still water level were –2.38 m, -1.46 m, -0.55 m, and +0.37 m, respectively. Irregular wave conditions were near depth-limited breaking at the wall for many of the tests. Zeroth-moment significant wave heights (H_{mo}) varied between 1.5 and 3.7 m, and the wave period associated with the peak of the wave spectrum (T_p) varied between 7.0 and 13.5 sec. Experiments were conducted without current and with seaward-flowing average current of 0.9 and 1.8 m/sec (prototype-scale units).

2.2 Measurements. The key measurements of these experiments were the incoming waves and the resultant forces on the overtopped vertical wall. Capacitance wave gauges recorded variations in the water surface elevation at a 20-Hz rate throughout the entire 360-sec duration of each experiment. Number of waves per experiment varied between 190 and 360 waves, depending on wave period. Wave data were collected near the 24-m-long wavemaker, at a three-gauge array just seaward of the vertical dike, shoreward of the vertical dike, and at a gauge on the same depth contour as the array but far enough to the side to be free of waves reflected by the wall. This latter gauge provided the incident wave parameter estimates. Frequency domain wave parameters were used in the analyses presented in this paper.

Wave forces on the vertical dike were measured using the apparatus shown in the center photograph in Figure 2. This force-measuring portion is the cantilevered wall section supported by the vertical framework. Narrow gaps separate the supported wall section from

the adjacent fixed wall. Wave forces applied over the wall section result in reactions at the upper supports as illustrated by the free-body diagram in Figure 2. Two force transducers were used at the fulcrum point (F_2 and F_3) and a third transducer was used at the top (F_1). Analysis of the free-body diagram at any time yields the total wave force F_L and the corresponding moment arm L_F about the wall base at that instant.

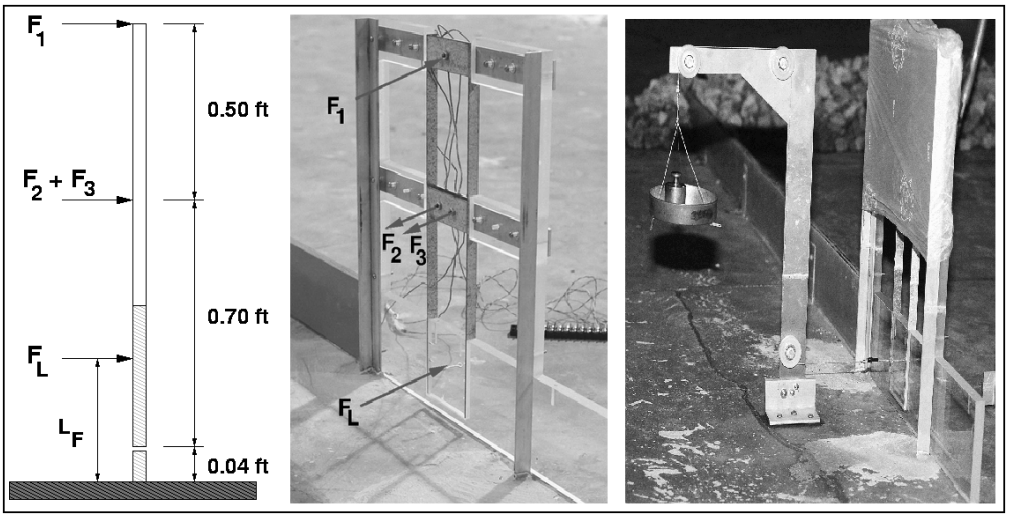

Figure 2. Force measuring section of model vertical dike

The force transducer cells were calibrated over the range of expected loading using pure axial loading. At the start and end of each day of testing the force-measuring device calibration was checked in place by affixing a calibration jig, as shown in the right-hand photo of Figure 2, and applying a series of known loads in the tray. This exerted a horizontal load on the wall section of known force and moment arm from which forces on the load cells could be checked. (Calibration checking was done with water in the model to assure any buoyancy forces were included.) Calibration loads were applied in both the shoreward and seaward directions. The calibration check revealed a small "residual resistance moment" in the force-measuring section caused by rigid connections between the supports and the load cells. The free-body analysis assumes frictionless pin connections. Calibration measurements were used to quantify the residual moment as an empirical equation over the range of loadings so that it could be removed from experiment force measurements.

Prior to the start of waves for each experiment the load cells were "zeroed" to show no force on the wall. For those experiments with constant seaward current, the current was allowed to reach a quasi-steady flow state before the force transducers were set to zero. Thus, forces recorded for each experiment represent the loading due solely to wave motions. After resetting the force transducers, waves were generated in the model; and shortly after the first waves reached the vertical wall, force data collection was started. Force data were collected from the three load cells at a 40-Hz rate for the same 360-second time period as the wave data. This logging rate was sufficient for recording pulsating wave loads, but the rate was not high enough to record impact loads. Because the top elevation of the wall was well beneath the wave crest elevation, impact loading was much less probable than for emergent walls.

2.3 Force Data Analysis. For each experiment the three synchronous force time series were first converted to engineering units (grams) and then combined at each time step according to the force balance equations derived from the free-body diagram of Figure 2. This resulted in time series of the total force on the force-measuring section (F_L) and the corresponding moment arm about the seabed (L_F). The residual moment was included in the moment arm calculation. Model force values were divided by the horizontal width of the force section to give force per unit length, and appropriate scale and conversion factors were applied to yield prototype-scale force per unit length in English units. The force time series exhibited characteristic sharp peaks in the shoreward direction (defined as negative) corresponding to the wave crests, and broad lower peaks in the seaward direction (positive) resulting from the passage of the wave trough over the wall.

Design of heavily overtopped vertical walls requires estimates of the largest forces and moments for a specified wave condition. For each time series the shoreward-directed and seaward-directed peak forces were extracted and plotted as distributions normalized by the root-mean-squared of the peak forces (F_{rms}) for the time series. Similarly, the distributions of shoreward- and seaward-directed peak moments were determined as the product of peak force and corresponding moment arm. Summary statistics from time domain analysis of the shoreward- and seaward-directed peak forces and moments were tabulated, plotted, and inspected for obvious trends. Forces and moments were always larger in the shoreward direction, and magnitudes increased with higher wall top elevation, higher zeroth-moment wave height, and longer peak wave periods. The effect of the seaward-directed current only caused a minor reduction in wave force on the vertical wall, and the current effect is not discussed further in this paper. However, the current does exert a seaward-directed steady force on the vertical wall that needs to be considered in design.

3. Force Distributions

Figure 3 shows typical results of the force and moment distributions. The upper and lower plots on the left side of Figure 3 show the shoreward- and seaward-directed normalized force distributions. The solid curve is the Rayleigh distribution based on the value of F_{rms} for the force peak distribution. The shoreward-directed peak force distribution is well represented by the Rayleigh distribution whereas the seaward-directed force distribution is a poorer match. This trend was characteristic of all the experiments. The upper and lower plots on the right side of Figure 3 present the corresponding distributions of peak moment for the experiment.

The prospect that the shoreward-directed peak force distribution can be reasonably approximated by the Rayleigh distribution based on the root-mean-squared peak force is a compelling concept to pursue because correlation of F_{rms} to parameters of the incident waves will likely be more successful than correlations based on extremes of the force distributions.

Figure 4 compares actual shoreward-directed peak force distribution parameters $F_{1/3}$ and $F_{1/10}$ to estimates using the Rayleigh distribution based on F_{rms} (where $F_{1/3}$ and $F_{1/10}$ are the average of the highest 1/3 and highest 1/10 of the force peaks, respectively).

Estimates of $F_{1/3}$ were quite good with little scatter around the line of equivalence. The most variation was for the largest forces observed at the wall with top elevation +0.37 m (prototype scale) above the still water level. More scatter was seen for estimates of $F_{1/10}$ as seen on the right side plot in Figure 4; however, the variation is not large, and it appears to be evenly distributed about the line of equivalence.

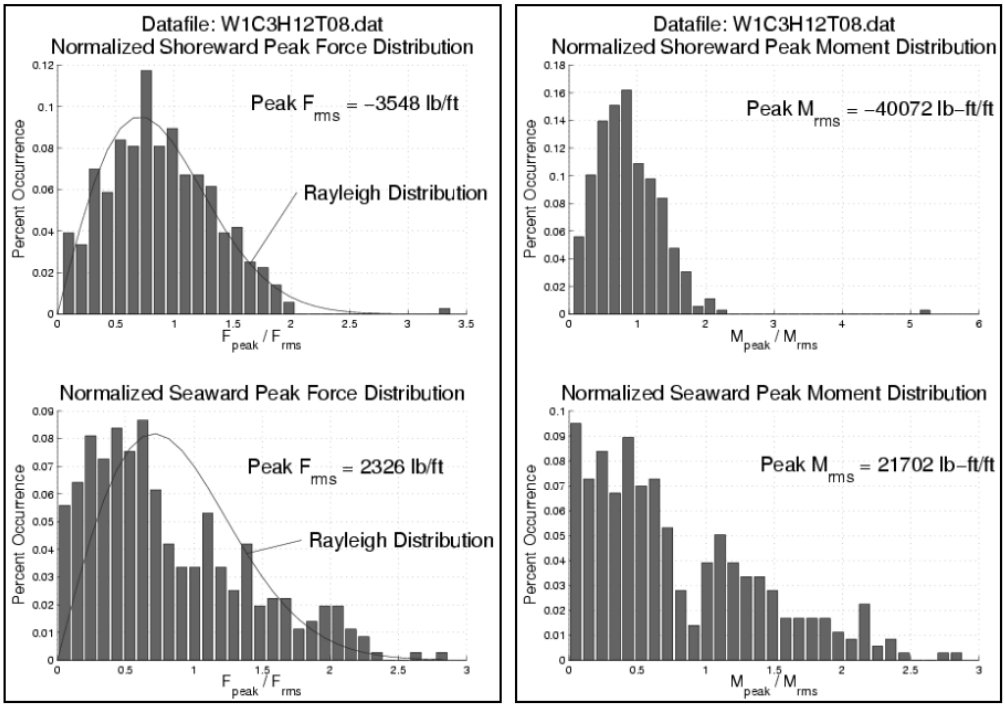

Figure 3. Representative distributions of shoreward and seaward peak forces and moments

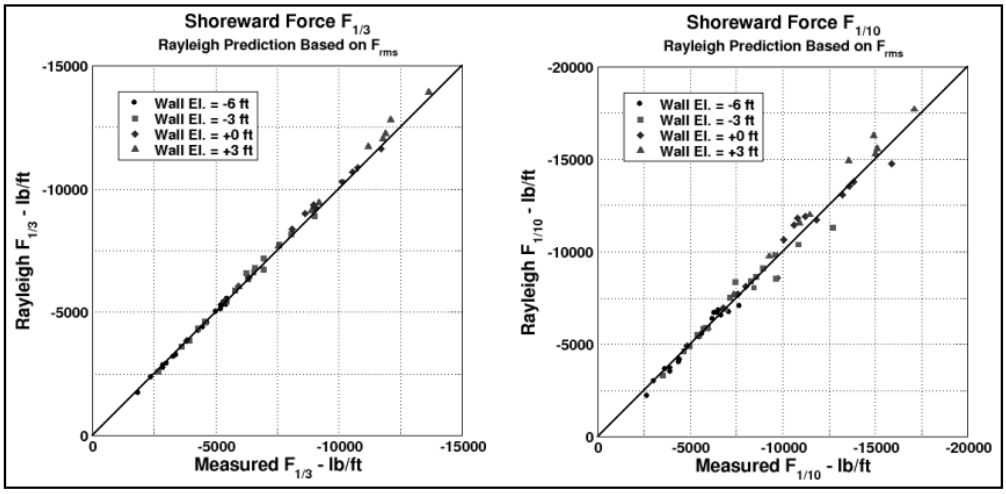

Figure 4. Shoreward-directed peak force Rayleigh prediction based on measured root-mean-squared force

Given the results shown in Figure 4, design guidance developed in this study was based on estimating the shoreward-directed root-mean-squared force F_{rms}, and then using the Rayleigh distribution to estimate extreme peak forces for the wave condition.

4. RMS Force Prediction

The force parameter representing the root-mean-squared values of the shoreward-directed peak forces (in English prototype units) is plotted versus the relative depth in Figure 5. Because the water level was the same for all experiments, the abscissa on the Figure 5 plot essentially shows only variation of peak spectral wave period.

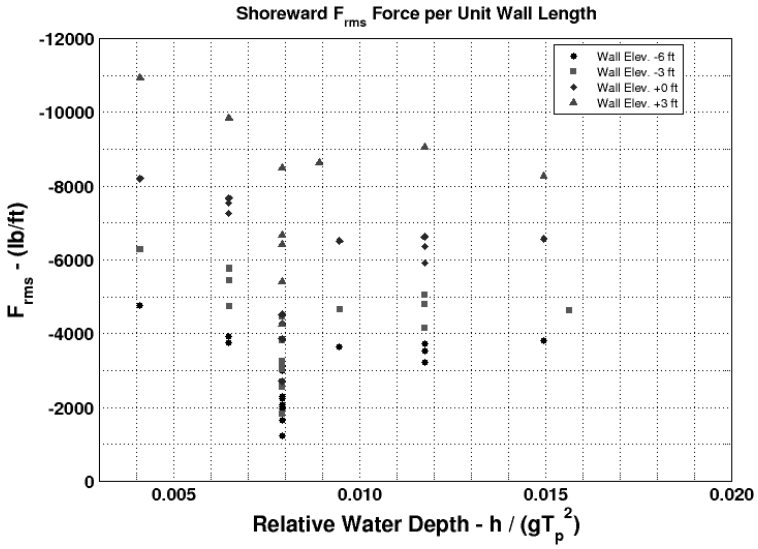

Figure 5. Root-mean-squared force versus relative water depth for all experiments

The RMS peak force increased with increasing top wall elevation, and relative wall height appeared to be the most influential test parameter. The F_{rms} force also increased gradually as the peak spectral wave period increased (decreasing relative water depth). Most experiments were conducted with waves approaching depth-limited breaking, and the RMS force increased as the wave height increased. However, experiments conducted with lower wave heights introduced additional scatter into the observed trends as seen in Figure 5 at relative water depth equal to about 0.0078. Out-flowing river currents had a relatively minor effect on the force results, and thus, current has been neglected in this analysis.

The next step was to normalize the RMS peak force values by an appropriate factor that accounted for the effects of wall height, water depth, wave height and wave period. This factor was derived by considering the trapezoidal wave-only peak force distributions shown in Figure 6.

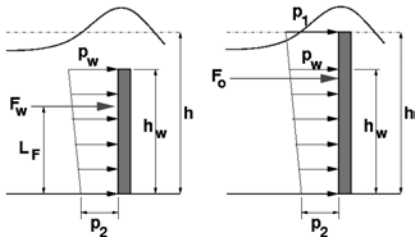

Figure 6. Definition sketch for wave-only trapezoidal force distributions on vertical walls

Equations for the total force on the submerged wall (left side of Figure 6) and the wall extending up to the still water line (right side) can be written in terms of the pressures and vertical dimensions. By further assuming the force distribution for the wall on the right side of Figure 6 is a linear extension of the distribution shown on the wall on the left side of the figure, it is possible to derive an expression for the force F_w in terms of F_o , p_2 , and the vertical heights, i.e.,

$$F_w = F_o\left(\frac{h_w}{h}\right)^2 + p_2\, h_w\left(1 - \frac{h_w}{h}\right) \qquad [1]$$

The first term in Eq. [1] dominates for vertical walls with top elevation near the still water level, and this suggests that $F_o / (h_w/h)^2$ might be a good normalizing factor for F_{rms} .
There are several ways to estimate the value of F_o . Three methods were considered:

- F_o is proportional to F_o estimated from linear wave theory
- F_o is proportional to F_o estimated using Goda's (1974) method for forces on walls
- F_o is proportional to the total nonlinear wave momentum flux at the wave crest

All three estimates for F_o in the normalizing factor gave reasonable results. However, estimates of F_o based on linear wave theory (e.g., Dean and Dalrymple 1984) and calculated using the Goda method resulted in a normalized peak RMS force that still exhibited an increasing trend with increasing wave period. This is probably related to increasing wave nonlinearity that is not captured by the first two methods. However, the wave nonlinearity was better represented when F_o was assumed to be proportional to total nonlinear wave momentum flux, M_F.
Hughes (2004) presented empirical equations to estimate the total depth-integrated wave momentum flux at the wave crest in terms of the relative wave height and relative water depth. For irregular waves the following formula for M_F was recommended.

$$\left(\frac{M_F}{\rho g h^2}\right)_{max} = A_0\left(\frac{h}{gT_p^2}\right)^{-A_1} \qquad [2]$$

where

$$A_0 = 0.639\left(\frac{H_{mo}}{h}\right)^{2.026} \qquad [3]$$

$$A_1 = 0.180\left(\frac{H_{mo}}{h}\right)^{-0.391} \qquad [4]$$

and h is water depth, ρ is water density, and g is gravitational acceleration.

Figure 7 presents the shoreward-directed normalized root-mean-squared peak wave force using nonlinear wave momentum flux in the normalizing factor. The relative wall height parameter accounts for much of the scatter reduction, and the wave momentum flux parameter seems to have accounted for wave nonlinearities because the data no longer exhibit an increase with wave period. The most scatter occurs at the wave period (10 sec prototype) where additional tests were conducted with smaller wave heights. One reason for the scatter could be associated with reduced flow separation as the smaller waves pass over the top of the wall.

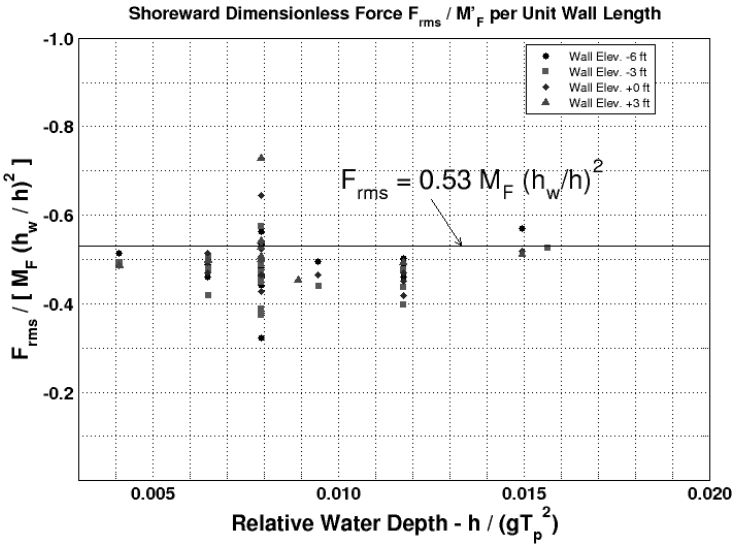

Figure 7. Shoreward-directed normalized RMS peak wave force versus relative water depth

The solid horizontal line in Figure 7 was drawn as a conservative recommendation for estimating the shoreward-directed RMS peak wave force acting on the overtopped vertical wall. This resulted in the following simple equation for estimating F_{rms}

$$F_{rms} = 0.53\, M_F \left(\frac{h_w}{h} \right)^2 \qquad [5]$$

where M_F is calculated using the formulas given in Eq. [2] – [4]. Because most of the experiments were conducted with waves approaching the depth-limiting condition, Eq. [5] may not be appropriate for smaller waves in deeper water.

5. Moment Arm Prediction

For each experiment the variation of calculated moment arm L_F associated with the peak shoreward-directed wave forces was examined. The moment arm was reasonably constant over most of the peak force range, so an average value was selected for each experiment. Figure 8 plots the relative moment arm versus relative water depth. For reference, uniform and triangular force distributions would have values of L_F/h_w equal to 0.5 and 0.67, respectively. The relative moment arm increased as the top wall elevation decreased relative to water depth indicating a nonlinear force distribution with most of the horizontal force load

being applied near the top of the wall. This increase may be related to flow separation as the wave passed over the wall. The relative moment arm also increased with increasing wave period.

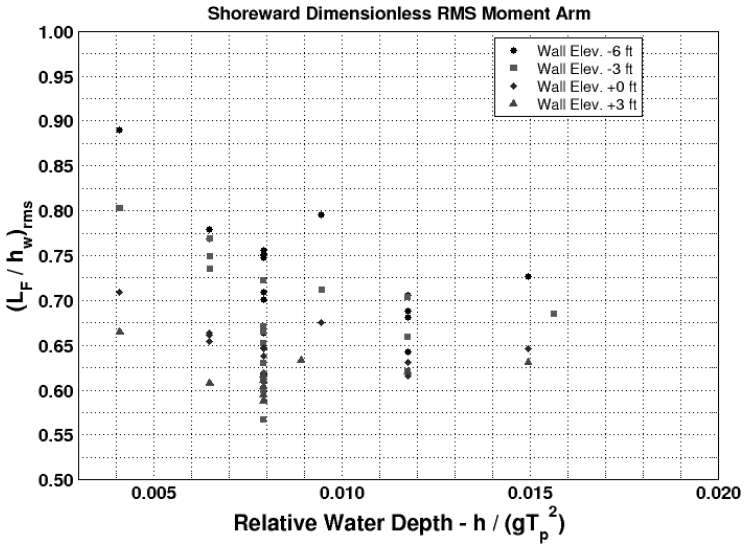

Figure 8. Relative shoreward-directed moment arm associated with peak wave forces

An appropriate normalizing factor was found by trial and error that yielded a strictly empirical formula that gives a conservative estimate of the moment arm as a function of water depth, wall height, and peak wave period, i.e.,

$$L_F = 0.4\, h_w \sqrt{\frac{h}{h_w}} \left(\frac{h}{g T_p^{\,2}} \right)^{-0.1} \qquad [6]$$

Figure 9 shows the final normalization that led to Eq. [6].

6. Conclusions

Wave forces on heavily overtopped vertical walls were measured for differing wall heights and wave conditions. The shoreward-directed forces were the largest, and the data indicated the distribution of the force peaks is well represented by the Rayleigh distribution based on the root-mean-squared force. An empirical equation was developed in terms of relative wall height and wave momentum flux to estimate the shoreward-directed RMS peak force. The associated moment arm, which is nearly constant over most of the peak force distribution, was also given by an empirical equation. For design application, first estimate the RMS peak force, then use the Rayleigh distribution to obtain an appropriate design force (e.g., $F_{1/100}$), and finally estimate the moment as the product of the force and moment arm using Eq. [6].

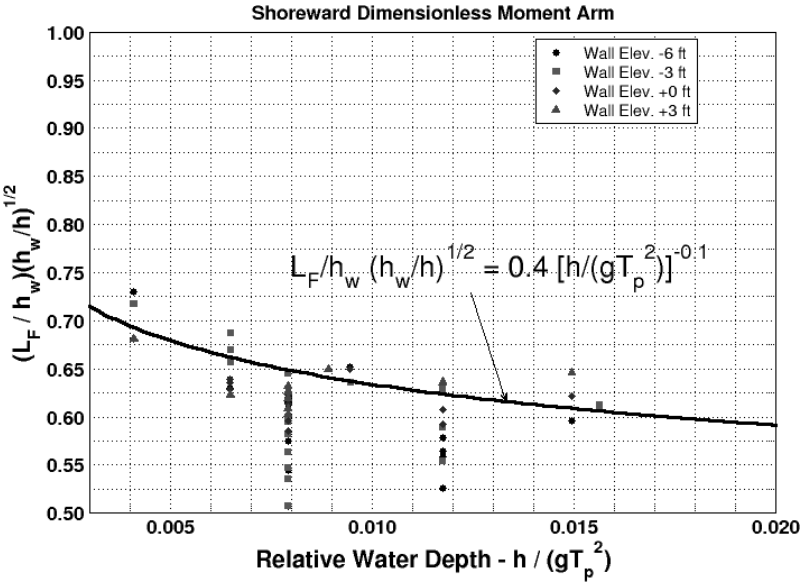

Figure 9. Normalized relative moment arm associated with shoreward-directed peak wave force

Acknowledgments

The study described and the results presented herein, unless otherwise noted, were obtained from research funded by the New Orleans District, US Army Corps of Engineers, and by the Coastal Inlets Research Program at the US Army Engineer Research and Development Center, Coastal and Hydraulics Laboratory. Permission was granted by Headquarters, U.S. Army Corps of Engineers, to publish this information.

References

Dean, R. G., and Dalrymple, R. A. 1984. 'Water Wave Mechanics for Engineers and Scientists,' Prentice-Hall, Inc., Englewood Cliffs, New Jersey. ISBN 0-13-946038-1.

Goda, Y. 1974. 'New wave pressure formulae for composite breakwaters,' *Proceedings of the 14th International Coastal Engineering Conference*, Vol 3, pp 1702-1720.

Hughes, S. A. 2004. 'Wave momentum flux parameter: a descriptor for nearshore waves,' *Coastal Engineering*, Vol 51, No. 11, pp 1067-1084.

Knott, G. F., and Mackley, M. R. 1980. 'On eddy motions near plates and ducts induced by water waves and periodic flows,' Phil. Trans. of the Royal Society, Vol 294, pp 599-628.